# Nonlocal approach to the analysis of the stress distribution in granular systems. II. Application to experiment

J. E. Scott and V. M. Kenkre
*Center for Advanced Studies, Department of Physics and Astronomy, University of New Mexico, Albuquerque, New Mexico 87131*

A. J. Hurd
*Sandia National Laboratories, Albuquerque, New Mexico 87185*
(Received 15 October 1997)

A theory of stress propagation in granular materials developed recently [Kenkre, Scott, Pease, and Hurd, preceding paper, Phys. Rev. E **57**, 5841 (1998)] is applied to the compaction of ceramic and metal powders in pipes with previously unexplained experimental features such as nonmonotonic density and stress variation along the axis of cylindrical compacts. [S1063-651X(98)14505-1]

PACS number(s): 81.05.Rm, 61.43.Gt, 81.20.Ev

## I. BACKGROUND AND ESSENTIAL FEATURES OF EXPERIMENTAL OBSERVATIONS

Although the study of granular systems has recently become a topic of intense discussion [1,2], the theoretical analysis of the stress behavior in bounded systems such as in powder metallurgical dies and ceramic compacts has been limited to simplified physical arguments concerning the transmission of stress into the walls of the confining system [3–5]. While such discussions provide a physical picture of how stress in granular systems propagates, they do not provide for a calculation of observed features. Recent experimental results [6], as well as data that have been available in the literature for many years [7–10], show unique features that have remained up to now unexplained. The present paper is an attempt to address such features with the help of a recently constructed theoretical framework [11]. Essential features of experimental observations are described in the rest of this section. A brief reminder of available theoretical approaches appears in Sec. II. We extend the theoretical framework of Ref. [11] to treat realistic depth-dependent boundary conditions and compare predictions of the theory to observations in Sec. III. In Sec. IV we investigate the importance of invoking a spatially nonlocal framework that is characteristic of our theory. Concluding remarks appear in Sec. V.

Generally, two approaches have been used to obtain experimental information about the propagation of stress in a powder compact: (1) direct measurement of the stress at points within a compact, and (2) direct mapping of the density distribution within a compact. The first approach involves the use of pressure sensors or strain gauges within, or at the edge of, a compact to measure the forces that evolve during pressing. Such measurements are limited by their accuracy and the ability of such gauges to measure the direction and location of the transmitted stress. The second approach relies on the assumption that the density at a point in a compact is related to the magnitude of the transmitted applied stress at that point. Various forms of relations exist to describe density-pressure behavior for granular systems [12–15].

Stress distribution observations include the experiments of Duwez and Zwell [16] who measured the pressure at the side wall of a cylindrical compact of copper powder as a function of depth. The side pressure was found to decrease linearly with distance away from the surface where the pressure was applied. Train [9] placed strain gauges within a fill of magnesium carbonate powder in a cylindrical die and measured the distribution of transmitted stress as a function of applied pressure during the compaction process. Along the centerline of the compact, the transmitted stress was observed to be a nonmonotonic function of the depth.

The measurement of density distributions is exemplified by the work of Kamm, Steinberg, and Wulff [7] who placed a thin lead grid into a cylindrical copper powder fill, which was subsequently pressed. The distortion of the grid was observed using x rays to determine the local variations in the density distribution of the compact. High and low density regions were observed along the centerline of the compact, while the density at the edge of the compact decreased from high density in the upper corners to low density at the bottom. Kuczynski and Zaplatynskyj [8] determined the density distribution of a nickel powder compact by sectioning it and testing the hardness of the compacted material as a function of location on the face of the section. By assuming a relation between the density of the material to its hardness, a density distribution was produced showing behavior similar to that seen by Kamm *et al.* [7]. The density along the top surface of the compact had a minimum in the center and increased to a maximum value at the edge of the compact. Train [9] measured the density distribution of the magnesium carbonate compacts that he used in his direct stress measurements by machining away sections and measuring the weight and volume of the material removed. Contour plots of the density distribution were produced showing the density for several different applied pressures. Well defined regions of high and low density along the centerline were observed, as well as the decreasing density along the edge of the compact. Macleod and Marshall [10] compacted uranium dioxide

 

powder in a cylindrical die for various applied pressures, then sectioned the compacts and placed them on photographic plates. Density distributions were obtained using contact autoradiography, where the exposure was calibrated by comparison with the optical density of plates that were exposed to uranium dioxide pellets with known densities. The contour plots they presented showed nonmonotonic behavior along the centerline of the compacts, with several regions of high and low density. Along the top surface, the density was a function of radius, increasing from a minimum at the center to a maxiumum at the edge of the compact, similar to the observations of Kuczynski and Zaplatynskyi [8]. Recently, Aydin, Briscoe, and Sanliturk [6] imbedded small lead balls in an alumina powder compact and used a technique similar to that of Kamm *et al.* [7] to determine the density distributions. Again, regions of high and low density were observed on the centerline, with the density at the edge of the compact decreasing with depth. Along the top surface of the compact, the density distribution, as a function of the radius, exhibited a minimum at the centerline and increased toward the edge of the compact, consistent with previous observations [8,10].

From the experimental data found in the literature, and the widely accepted notion [17] that the spatial variation of the density follows, in essence, the spatial variation of the stress, three essential features describing the stress distribution in compacts can be inferred: (1) the applied stress at the top surface is not constant, but increases from a minimum at the center to a maximum at the edges, (2) the stress at the edges decreases with depth from the surface where the pressure is applied, and (3) the stress along the centerline is a nonmonotonic function of depth, with well defined regions of low and high stress. These features, which are common to observations made in a variety of powders over a wide range of applied pressures, provide inputs, as well as a test for theoretical treatments of the stress distribution in compacts: no theoretical analysis known to us has adequately addressed the appearance of nonmonotonic stress behavior along the axis.

## II. DISCUSSION OF AVAILABLE THEORETICAL ANALYSES

A number of theoretical approaches have been developed to describe the stress behavior in granular systems. Janssen [18] developed a theory that reproduced an exponential decrease along the walls of a silo. That theory was modified by Thompson [13] to apply to ceramic powder compacts, but was unable to reproduce the nonmonotonic behavior along the centerline. Edwards and collaborators [3,4] mathematically described ''stress arches'' that are believed to carry the stress to the walls of a pipe, but did not extend their theory to stress distributions within powder compacts. Bouchaud *et al.* [5] proposed wavelike behavior for stress in granular systems, and Liu *et al.* [19] investigated a diffusive model [20]. These were primarily interested in the calculation of the stress in sandpiles and did not produce stress maps for powder compacts. Aydin *et al.* [6] used a nonlinear stress-strain constitutive relation in a finite-element calculation to produce stress distributions that were similar to experimental results, but failed to reproduce the observed density peak along the compact centerline.

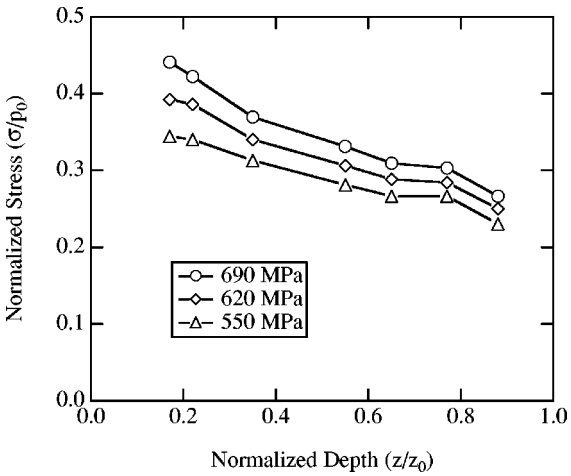


FIG. 1. Measured stress at the edge of a cylindrical compact normalized to the average applied pressure and plotted as a function of depth in the compact (taken from Duwez and Zwell [16]). This supports the use of a monotonic function to describe the stress at the walls.

Our theory [11] [Kenkre, Scott, Pease, and Hurd (KSPH)] based on considerations [21,22] similar to those employed in theories of exciton dynamics unifies the work of Bouchaud *et al.* [5] and Liu *et al.* [19] through the use of a spatially nonlocal constitutive relation between the stress $\sigma_{zz}(x,y,z)$ and a ''stress flux'' $j(x,y,z)$, which is composed of the shear components of stress in the plane perpendicular to the $z$ direction, along which the compaction pressure is applied. The unification allows the KSPH theory to retain elements of the light cones of Bouchaud *et al.* and their identification with the arches of Edwards and co-workers [3,4] yet to incorporate some of the random stress transmission of Liu *et al.* that must accompany a realistic picture of the random packing in granular systems. The present paper consists of an extension of KSPH theory to address boundary conditions of relevance to experiment and of an application of the theory to several experimental observations in the literature.

## III. EXTENSION OF THE KSPH THEORY FOR REALISTIC BOUNDARY CONDITIONS AND COMPARISON TO EXPERIMENT

As in Ref. [11], we will restrict our analysis to two dimensions $(x,z)$ for simplicity. For the illustrative boundary condition where $\sigma_{zz}(\pm L/2,z)$ vanishes, the solution of the telegrapher's equation for symmetric compacts has been given in Ref. [11] as

$$\sigma_{zz}(x,z)=\sum_k A_k g_k(z)\cos kx, \tag{3.1}$$

where

$$g_k(z)=e^{-(\alpha/2)z}\left[\cosh \Omega_k z+\frac{\alpha}{2\Omega_k}\sinh \Omega_k z\right],$$

$$\Omega_k=\sqrt{\alpha^2/4-c^2k^2} \tag{3.2}$$

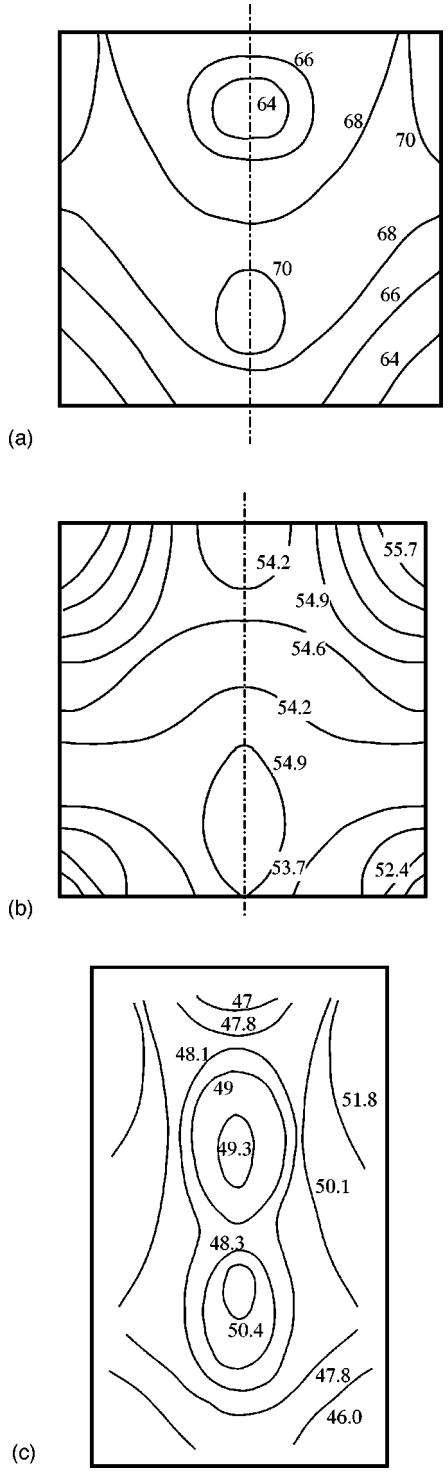


FIG. 2. Density distribution (in percent solid density) for cylindrical compacts of (a) magnesium carbonate powder pressed at 200 MPa (taken from Train [9]), (b) alumina powder pressed at 38.6 MPa (taken from Aydin *et al.* [6]), and (c) uranium dioxide powder pressed at 160 MPa (taken from Macleod and Marshall [10]).

and

$$k=(2m+1)\frac{\pi}{L}, \quad m=0,1,2,\ldots . \tag{3.3}$$

The Fourier coefficients are determined by the applied pressure on the top surface, $\sigma(x,0)$:

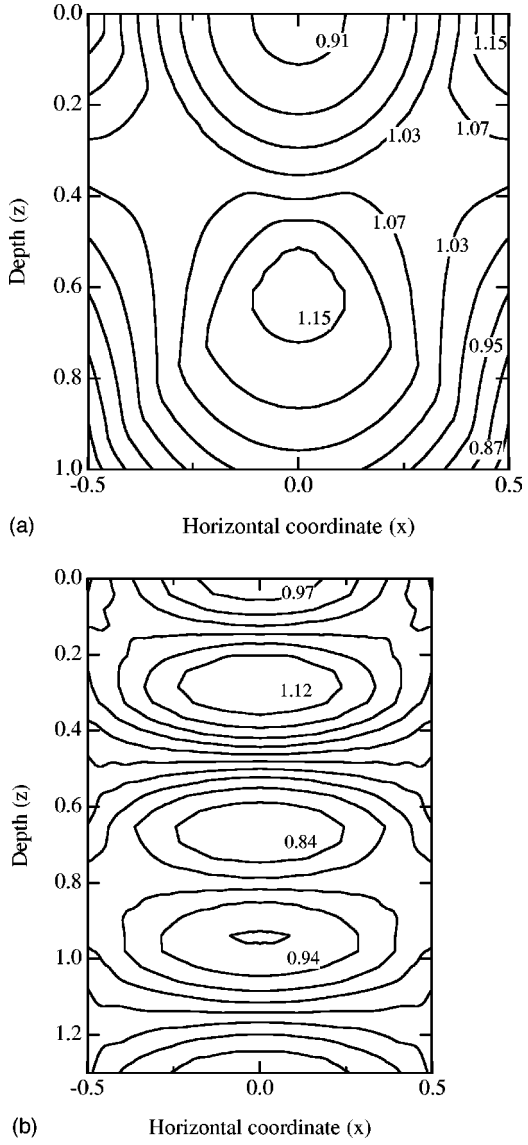


FIG. 3. Stress distributions calculated using Eq. (3.13) with $p_0=1.0$, $L=1.0$, and $\beta=0.5$ with (a) $c=1.0$, $\alpha=1.0$, $\gamma=0.8$, and $c_0=0.90$, and (b) $c=3.0$, $\alpha=0.9$, $\gamma=0.5$, and $c_0=0.95$. The numbers represent the magnitude of the normalized stress, $\sigma/p_0$. Units are arbitrary.

$$A_k=\frac{2}{L}\int_{-L/2}^{L/2}dx\ \ \sigma(x,0)\cos\, kx. \tag{3.4}$$

In the present paper, our interest is in obtaining stress distributions for systems with realistic rather than illustrative initial and boundary conditions. Therefore, we do not take $\sigma_{zz}(\pm L/2,z)$ to vanish, but rather to be a given function $h(z)$ of the depth:

$$\sigma_{zz}(x,z)\big|_{x=\pm L/2}=p_0h(z), \tag{3.5}$$

where $p_0$ is the average value of the applied stress at the top surface. The solution of the telegrapher's equation with such initial and boundary conditions presents an unusual boundary value problem that is analogous to propagation problems in which the boundary condition is dependent on time [23]. Generalizing Eq. (3.1) to this case as

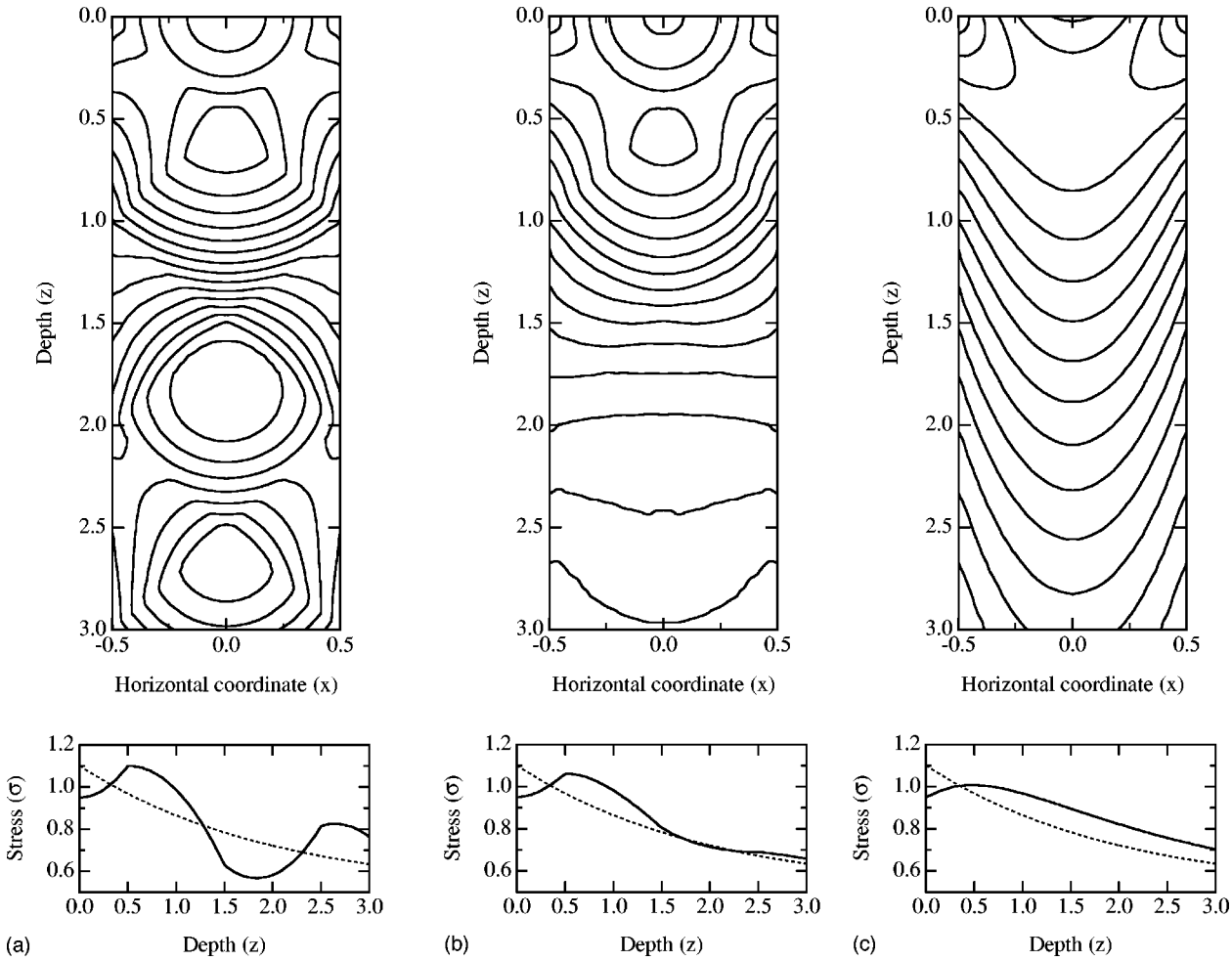


FIG. 4. Calculated stress distributions using Eq. (3.13) showing the transition from fully wavelike stress propagation to diffusive propagation. The plots below the contour plots show the centerline stress compared to the exponential boundary condition. Here $p_0=1.0$, $L=1.0$, $\beta=0.5$, $\gamma=0.5$, and $c_0=0.95$ with (a) $c=1.0$, $\alpha=0.0$, (b) $c=1.0$, $\alpha=2.0$, (c) $c=13.0$, $\alpha=1000$. Units are arbitrary.

$$\sigma_{zz}(x,z)=\sum_k A_k G_k(z)\cos(kx) \tag{3.6}$$

we obtain

$$\frac{\partial^2 G_k(z)}{\partial z^2}+\alpha\frac{\partial G_k(z)}{\partial z}+c^2k^2G_k(z)=c^2k^2b_m h(z), \tag{3.7}$$

where $b_m=p_0a_m/A_k$ with

$$a_m=\frac{4(-1)^m}{\pi(2m+1)}, \quad m=0,1,2,\ldots. \tag{3.8}$$

Equation (3.7) is solved explicitly as

$$G_k(z)=g_k(z)-b_m\int_0^z dz' h(z-z')\frac{\partial g_k(z')}{\partial z'}. \tag{3.9}$$

Here $k$ and $m$ are defined in Eq. (3.3) and $A_k$ is defined in Eq. (3.4).

In a manner analogous to that used in the treatment of Thompson [13], we take the applied stress at $z=0$ to have a parabolic dependence:

$$\sigma(x,0)=p_0\left(c_0+(1-c_0)\frac{12x^2}{L^2}\right). \tag{3.10}$$

Here, $c_0=\sigma(0,0)/p_0$, which ensures that the integrated applied pressure is equal to $p_0$. Evaluating Eq. (3.4), we obtain

$$A_k=p_0a_m\left[c_0+3(1-c_0)\left(\frac{k^2L^2-8}{k^2L^2}\right)\right]. \tag{3.11}$$

Equations (3.6) and (3.9), along with (3.2) and (3.11), constitute the result of Ref. [11] extended to realistic initial and boundary conditions. In our further calculations, the functional form of $h(z)$ will be taken to follow experimentally observed stress behavior at the walls. A typical set of observations taken from Duwez and Zwell [16] is plotted in Fig. 1 showing the stress at the boundary decreasing with increasing depth. One way to model this is to take $h(z)$ to be an exponentially decreasing function:

$$h(z)=\beta+[(3-2c_0)-\beta]e^{-\gamma z}. \tag{3.12}$$

Solving Eq. (3.9), we obtain for the propagating stress

$$\sigma_{zz}(x,z)=p_0\beta+\sum_k (A_k-p_0a_m\beta)g_k(z)\cos kx + p_0[(3-2c_0)-\beta]\sum_k \frac{c^2k^2a_m}{(\gamma-\alpha/2)^2-\Omega_k{}^2} \times\left\{e^{-\gamma z}-g_k(z)+\frac{\gamma}{\Omega_k}e^{-(\alpha/2)z}\sinh\,\Omega_k z\right\} \times\cos\,kx, \tag{3.13}$$

where $a_m$ and $A_k$ are defined in Eqs. (3.8) and (3.11), respectively.

The qualitative distribution of the stress in a compact can be visualized, as described previously, through the density distribution. We show here three such density distributions in Figs. 2(a), 2(b), and 2(c) as obtained by Train [9], Aydin *et al.* [6], and Macleod and Marshall [10], respectively. Data in Figs. 2(a) and 2(b), while referring to different materials under vastly different conditions, are similar to each other and exhibit high density regions in the upper corners of the compact, low density regions in the lower corners, and nonmonotonic behavior along the centerline. Figure 2(c) shows the intriguing observation of multiple regions of high and low density along the centerline. Our theory, as represented by Eq. (3.13), can describe the features in Fig. 2(c) as well as in 2(a) and 2(b). This is clear from a comparison of Figs. 2(a) and 2(b) with the results of our theory in Fig. 3(a), and of Fig. 2(c) with our result as shown in Fig. 3(b). One of the interesting features of KSPH theory [11] is that oscillatory behavior in the stress is predicted along the centerline of the compact as the result of the interference of reflected stress waves. Such behavior, apparent in the theoretical result, Fig. 3(b), appears to have been observed in Macleod and Marshall's compaction observations in uranium dioxide [see Fig. 2(c)].

Indeed, as a result of the underlying use of the telegrapher's equation, KSPH theory is able to describe the entire range of behavior from wavelike to diffusive ''propagation'' of stress. In order to display this wide range of applicability of KSPH theory, we plot in Fig. 4 a series of contour plots and centerline sections of the stress distribution as we change the parameters $c$ and $\alpha$. We note that the first maximum along the centerline arises merely from the propagation of the initial high stress regions in the upper corners into the interior of the compact and is not a result of wavelike behavior. The second maximum appears as an oscillation about the imposed boundary function and is present in Figs. 4(a) and 4(b), but not in Fig. 4(c) where the parameters approach the diffusive limit. This oscillation (second maximum) *is* a manifestation of the wave nature of the stress propagation. We also note that the magnitude of the first maximum along the centerline decreases in the transition from wave to diffusive propagation.

In Fig. 5 we display three-dimensional plots of the stress distribution in the two extreme limits corresponding to the contour plots in Figs. 4(a) and 4(c), respectively. The plot labeled ''wave limit'' corresponds to a vanishing value of $\alpha$, and the one labeled ''diffusive limit'' to $c,\alpha\rightarrow\infty$, $c^2/\alpha=D$. Although the authors of [5] and [19,20] did not carry out a boundary value analysis as we have done in Ref. [11] and the present paper, we will call these two extreme limits the Bouchaud and the Liu limits, respectively. In both cases, the characteristic parabolic variation of the pressure at the top surface of the die (farther into the paper) is quite clear. As in other treatments, this variation is an input to our theory. The propagation of the curvature into the compact is, however, determined by the theory. In both limits, one sees an inversion of the curvature as one goes towards larger depths. The inversion has been remarked on in the analysis of Thompson [13] as an observed feature, but to our knowledge no explanation of it exists in the literature. In both limits, as one progresses along the centerline down the die from the top surface, one encounters a maximum. However, the maximum is a true peak (maximum from all directions) only in the wave case. In the diffusive case the nature of the stress distribution is substantially different: only a ridge occurs. This important difference is reflected in the contour plots in the presence (absence) of closed contours in the wave (diffusive) limits. Additional maxima (oscillation) appear only in the Bouchaud limit and not in the Liu limit, and arise clearly from the wave ingredient of stress propagation via wall reflections.

## IV. IS IT NECESSARY TO INVOKE A NONLOCAL APPROACH?

The KSPH theory is based on a nonlocal constitutive relation [11] that results in the telegrapher's equation. We have shown above that it describes the qualitative features of the observations satisfactorily. However, it has also been shown in Ref. [11] that the evolution equation reduces in an extreme limit to the diffusion equation and therefore to considerations presented by Liu *et al.* [19]. In that analysis, the random propagation of stress from one particle to another is invoked—a condition that is appealing because of the random nature of the particle sizes, shapes, and locations. It is therefore natural to ask whether the diffusive limit would suffice to describe the observed stress distribution. We find an unequivocal answer to this question in the context of the experiments reported in Refs. [9,6,10]. Our reasoning is as follows.

The diffusive limit of our equation (3.13) is

$$\sigma_{zz}(x,z)=p_0\beta+\sum_k (A_k-p_0a_m\beta)e^{-Dk^2z}\cos\,kx+p_0[(3-2c_0)-\beta]\sum_k \frac{Dk^2a_m}{\gamma-Dk^2}\{e^{-Dk^2z}-e^{-\gamma z}\}\cos\,kx, \tag{4.1}$$

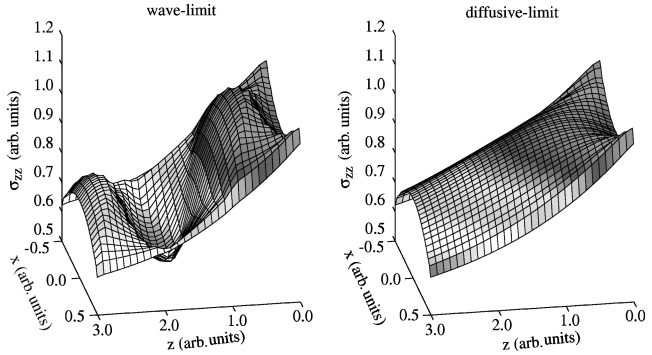


FIG. 5. Three-dimensional plots of the stress distribution calculated using Eq. (3.13) in the wave limit ($\alpha=0$), and in the diffusive limit ($c,\alpha\to\infty$, $c^2/\alpha=D$). Units are arbitrary.

where $a_m$ and $A_k$ are given by Eqs. (3.8) and (3.11), respectively. It is clear that it can predict no oscillations of stress with changes in depth since no oscillations in $z$ [no trigonometric functions as in Eq. (3.13)] appear in the right-hand side of Eq. (4.1). The wave ingredient of the telegrapher's equation is, thus, essential to explain the uranium dioxide data. Furthermore, even for the data on magnesium carbonate and alumina, which exhibit no such oscillations, a careful analysis based on our predictions discussed in Fig. 4 leads to the conclusion that the diffusive limit is inadequate. Crucial to this conclusion is the presence of true peaks, marked by closed contours, in the stress plots seen in all data displayed. Several such peaks are noticed in the extreme wave limit in Fig. 4(a). This wave tendency decreases as we progress from cases (a) through (c), as the stress evolution becomes increasingly more diffusive. Indeed, no peaks appear in the diffusive limit as Fig. 4(c) shows. This is also clearly shown in the three-dimensional plots of Fig. 5. We therefore conclude that there is a definite wave ingredient present in the stress distributions displayed in the experiments of Refs. [9,6,10].

For the sake of completeness, we have shown in Fig. 6 predictions of our theory in the diffusive limit (4.1). No closed contours occur. Increasing the value of the diffusion constant $D$ results in increased rate of diffusion of the wall boundary condition into the compact.

Can other existing calculations of the stress describe the experimentally observed features? To answer this question, we look at the calculations of Aydin *et al.* [6] who used a nonlinear stress-strain constitutive model in a discrete element calculation to obtain a density distribution that we reproduce here in Fig. 7. This calculation, using input from the

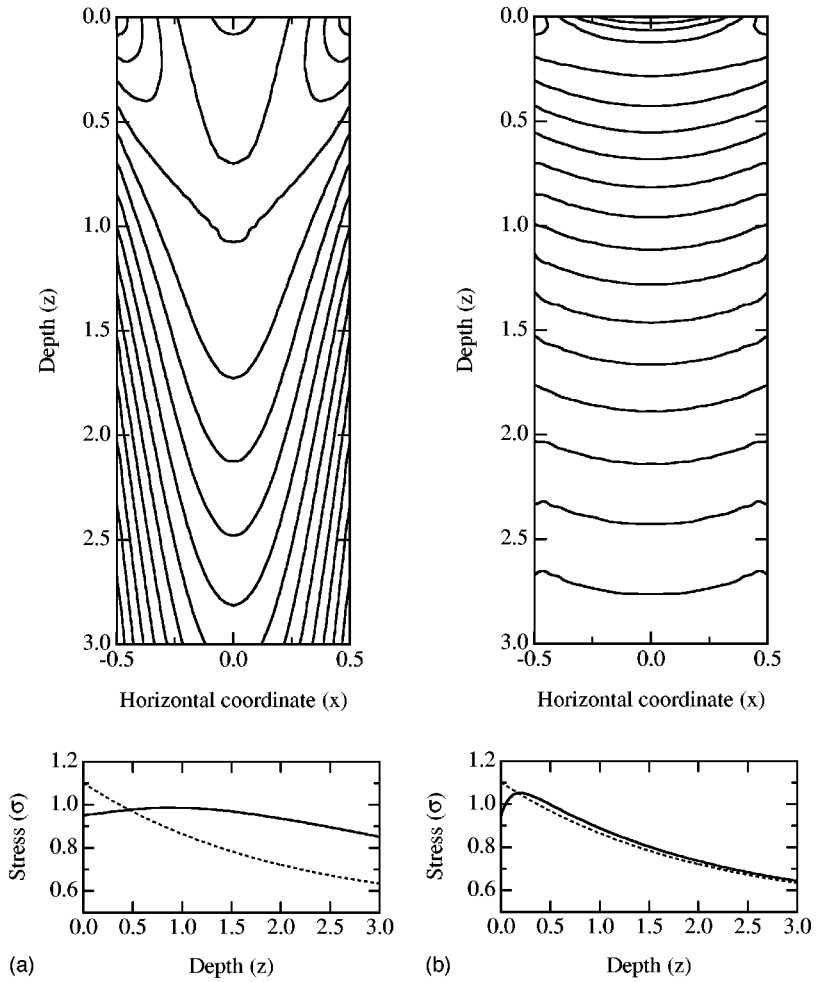


FIG. 6. Calculated stress distributions using Eq. (4.1) showing the effect of increasing the diffusion constant on the stress distribution. The plots below the contour plots show the centerline stress compared to the exponential boundary condition. Here $p_0=1.0$, $L=1.0$, $\beta=0.5$, $\gamma=0.5$, and $c_0=0.95$ with (a) $D=0.05$, and (b) $D=1.0$. Units are arbitrary.

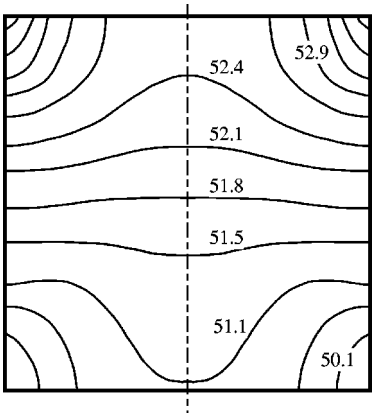


FIG. 7. Calculated density distribution (in percent solid density) from Ref. [6] corresponding to experimental conditions that produced Fig. 2(b).

experimental conditions used to obtain the plot shown in Fig. 2(b), compares favorably in that the regions of high and low density in the corners of the compact are calculated, but fails to predict the low and high density regions along the centerline. Aydin *et al.* [6] acknowledge this failure explicitly and suggest that it is due to the lack of inclusion of internal friction effects between the particles. We suggest that the constitutive relations postulated by Aydin *et al.* describe in detail the local interaction from one point particle to another, but do not describe long-range (nonlocal) correlations between particles.

## V. REMARKS

The primary conclusions to be drawn from the present investigation are that (1) experimental data in the literature clearly document nonmonotonic behavior in the stress along the axis of a cylindrical compact, as seen in direct observations of stress [9] as well as in observations of density distributions in compacts of metallic and ceramic powders [6–10]; (2) our theory, as developed in Ref. [11], and applied here to realistic boundary conditions, predicts this behavior; and that (3) wave aspects, as proposed by Bouchaud *et al.* [5], are essential to the understanding of the observations in Refs. [9,6,10]. The negativity problem mentioned in Ref. [11], i.e., that the calculation of the stress near the wave limit can result in negative stress for certain parameter values, has been addressed satisfactorily in the present paper by taking the observed stress along the walls as an input through an appropriate choice of the term $\beta$ in the boundary condition given by Eq. (3.12).

It is well known that wall lubrication plays a role in the development of the observed distribution of stress in a compact, but its role has remained a mystery. While we have not resolved this mystery, we have incorporated wall effects explicitly by taking $h(z)$ as an input. By changing the functional behavior of the stress at the boundaries, the predicted stress distribution is changed. The functional form of the boundary stress coupled with the finite ''speed'' of propagation through the granular medium manifests itself in the shape of the centerline maximum that is seen in experimental observations. This suggests that the stress distribution within a powder compact may be used to evaluate the functional form of the stress at the compact edge, and that in turn may provide insight into the behavior of the frictional interaction at the walls. That understanding may lead to specific wall lubrication schemes that can be implemented to minimize variations in the stress distribution.

With this demonstration of the ability of theory to predict experimental observables, we can make specific recommendations for further studies, including: (1) the detailed experimental measurement of the transmitted stress in the $z$ direction at the walls of a cylindrical compact with various wall lubrications schemes and their subsequent effect on the density (and stress) distribution throughout the compact, (2) the evaluation of these distributions using the KSPH theory [11] with boundary conditions that match the experimental observations, (3) the study of the effects of granular particle shape, composition, size distribution, packing density, etc. on various parameters in Ref. [11] such as $c$, $\alpha$, and in particular, on the functional form of the spatial memory itself. With such an understanding, it would be possible to predict the stress propagation in compacts from morphological measurement of granular particles, and, in that way, develop techniques to optimize the compaction process.

## ACKNOWLEDGMENT

This work was supported in part by Sandia National Laboratories under Department of Energy Contract No. DE-AC04-94A85000.

[1] H. M. Jaeger, S. R. Nagel, and R. P. Behringer, Rev. Mod. Phys. **68**, 1259 (1996); Phys. Today **49** (4), 32 (1996).
[2] *Granular Matter: An Interdisciplinary Approach*, edited by A. Mehta (Springer-Verlag, New York, 1994).
[3] S. F. Edwards and R. B. S. Oakeshott, Physica D **38**, 88 (1989).
[4] S. F. Edwards and C. C. Mounfield, Physica A **226**, 1 (1996).
[5] J.-P. Bouchaud, M. E. Cates, and P. Claudin, J. Phys. I **5**, 639 (1995).
[6] I. Aydin, B. J. Briscoe, and K. Y. Sanliturk, Comput. Mater. Sci. **3**, 55 (1994); Powder Technol. **89**, 239 (1996).
[7] R. Kamm, M. A. Steinberg, and J. Wulff, Trans. AIME **171**, 439 (1947); **180**, 694 (1949).
[8] G. C. Kuczynski and I. Zaplatynskyj, Trans. AIME **206**, 215 (1956).
[9] D. Train, Trans. Inst. Chem. Eng. **35**, 258 (1957).
[10] H. M. Macleod and K. Marshall, Powder Technol. **16**, 107 (1977).
[11] V. M. Kenkre, J. E. Scott, E. A. Pease, and A. J. Hurd, preceding paper, Phys. Rev. E **57**, 5841 (1998).
[12] R. P. Seelig, Trans. AIME **171**, 506 (1947).
[13] R. A. Thompson, Ceram. Bull. **60**, 237 (1981).
[14] A. R. Cooper and L. E. Eaton, J. Am. Ceram. Soc. **45**, 97 (1962).
[15] V. M. Kenkre, M. R. Endicott, S. J. Glass, and A. J. Hurd, J. Am. Ceram. Soc. **79**, 3045 (1996).

[16] P. Duwez and L. Zwell, Trans. AIME **185**, 137 (1949).
[17] Strong support for this assumption was given by Train in Ref. [9] who displays stress as well as density distributions for the same compacts.
[18] H. A. Janssen, Z. Ver. Dt. Ing. **39**, 1045 (1895).
[19] C.-h. Liu, S. R. Nagel, D. A. Schecter, S. N. Coppersmith, S. Majumdar, O. Narayan, and T. A. Witten, Science **269**, 513 (1995).
[20] S. N. Coppersmith, C.-h. Liu, S. Majumdar, O. Narayan, and T. A. Witten, Phys. Rev. E **53**, 4673 (1996).
[21] V. M. Kenkre, in *Energy Transfer Processes in Condensed Matter*, edited by B. Di Bartolo (Plenum Press, New York, 1984), pp. 205–249.
[22] V. M. Kenkre and P. Reineker, *Exciton Dynamics in Molecular Crystals and Aggregates* (Springer-Verlag, New York, 1982).
[23] S. J. Farlow, *Partial Differential Equations for Scientists and Engineers* (Dover Publications, New York, 1982), pp. 64–73.